PHYSICAL REVIEW A VOLUME 35, NUMBER 4 FEBRUARY 15, 1987

Generalized squeezing

Samuel L. Braunstein
California Institute of Technology (Theoretical Astrophysics 130-33), Pasadena, California 91125

Robert I. McLachlan
Department of Applied Mathematics (217-50), California Institute of Technology, Pasadena, California 91125
(Received 29 August 1986)

We consider a generalized form of parametric amplification which produces k-photon correlations. We show numerically that this process is well-defined quantum mechanically, and we explain the quantum phase-space structures produced by such parametric amplification.

I. INTRODUCTION

In this paper we discuss a generalization of squeezed states. Throughout this paper "squeezing" refers to ordinary squeezing, and the term "generalized squeezing" shall be used explicitly when referring to our work.

In experiments where all sources of external noise have been made insignificant, there are still limits in measurement precision due to the Heisenberg uncertainty principle. This uncertainty in the variables is like a "quantum noise." Now we can use an idealized prescription where a detector is coupled to a harmonic oscillator. This is quite a general prescription (e.g., the harmonic oscillator's coordinates could represent the electric field in light, or the position or momentum in a mass-spring system), so we shall restrict our attention to such systems. The quantum states which most closely describe the classical motion of these systems are harmonic oscillator coherent states. If we call the canonically conjugate variables for our harmonic oscillator system "position" x and "momentum" p, but choose appropriate dimensionless units for them, then the coherent states have a symmetric uncertainty in x and p with $\Delta x \Delta p = 1$ and $\Delta x = \Delta p = 1$.

A loose classical description of quantum states can be made in terms of a phase-space probability distribution. For coherent states this corresponds to a bivariate Gaussian distribution in x and p displaced from the origin and rotating around it with time. The rotation in phase space corresponds to the oscillation of p one quarter cycle ahead of x, and the equality of the uncertainties in x and p initially leads to both Δx and Δp being independent of time. Thus the harmonic oscillator coherent state has a time-stationary "noise."

Since the uncertainty principle only puts a restriction on the product $\Delta x \Delta p$ we might consider starting with a more precise position, so $\Delta x < 1$, and a more uncertain momentum, $\Delta p > 1$. These states are called squeezed states;[1] the noise has been squeezed into one variable at the expense of its conjugate. We see that as this state evolves freely in a harmonic oscillator potential the precise x rotates in phase space to become a precise p in one quarter cycle, and the uncertainty in p gets rotated into that of x. This variation of the uncertainty in these variables gives squeezed states a time-dependent noise (or as we shall refer to it in this paper a phase-dependent noise).

A simple change in the variable we observe can yield a time stationary noise for squeezed states. Roughly this change corresponds to measuring either x or p in a rotating frame in phase space. This new variable is called the quadrature phase (or quadrature amplitude), so squeezed states have a time stationary quadrature phase noise. In practice the quadrature phase is measured by interfering the original signal with an oscillating reference. This is just a homodyne or heterodyne detection scheme.

Real two-photon devices have recently been used to produce squeezed states of light.[2,3] With the use of these devices comes the promise of improved high-precision interferometers.[4–6]

Any states deserving the name "generalized squeezed states" should have properties analogous to ordinary squeezed states, they must reduce to ordinary squeezing appropriately, and they should be generated from a phenomenologically reasonable model. The first requirement is somewhat vague so we shall simply take it to mean that these new states should at least possess a phase-dependent noise. We concentrate on a class of devices that generate states satisfying these criteria.

In Sec. II such devices are modeled by ideal k-photon "parametric amplifiers" (creating or destroying k photons at a time) acting, for simplicity, on a single mode of the electromagnetic field. Ordinary squeezing corresponds to $k = 2$. This section also analyzes these devices in a qualitative classical manner and suggests why we expect them to generate phase dependent noise.

A simple but quantitative way to discuss the noise of these generalized squeezed states is through the use of a quantum analogue of the joint probability distribution in phase space. This analogue is known as the Q-function. We review this quantum description in Sec. III and derive some analytic properties that the Q-function of our k-photon state must satisfy. We find that the analytic properties of the Q-function closely follow our qualitative classical prejudices. In this section we also look at the asymptotic behavior, for short time, of the Q-function. For the case $k = 3$ we find that a large-amplitude coherent state is initially squeezed at a rate proportional to its amplitude—intrinsically much faster squeezing than that produced by ordinary squeezing interactions ($k = 2$).

In Sec. IV we study this classical-quantum correspondence more closely. We start by finding the proper classical Hamiltonian corresponding to these k-photon devices. Having set up the classical problem, we find that the classical and quantum evolution differ for $k>1$. The classical motion is determined by an unstable fixed point at the origin of phase space; the classical evolution is "driven" by this fixed point to produce very sharp features in the classical probability distribution. These sharp features are destroyed by the quantum corrections, the dominant terms of which correspond to ordinary diffusion when $k>1$.

Fisher, Nieto, and Sandberg[7] have also studied this generalization to squeezing via k-photon devices. They concluded that there is something seriously wrong with the evolution operator for these devices, after discovering that for $k>2$ its vacuum-to-vacuum matrix element has a divergent Taylor series expansion in time. In Sec. V we study this matrix element numerically using Padé approximants. We obtain good convergence for this matrix element for all scaled times (the coupling constant of the parametric amplifier multiplied by time) less than about 1.2. We also see that the divergence problems are due to singular behavior along the imaginary time axis. This matrix element and others are used to generate contour plots of the Q-function for $k=3$ and $k=4$ at various scaled times.

Hong and Mandel[8] have defined a set of parameters which they call measures of "nth-order squeezing" for even n. When $n=2$ this parameter reduces to a measure of the uncertainty in the quadrature phase, and so corresponds to a measure of ordinary squeezing. We calculate the second-order and fourth-order squeezing parameters for some of the three-photon and four-photon states we have generated, and we find that these states are neither ordinarily squeezed nor squeezed to fourth-order. Nonetheless, for the reasons already mentioned we consider our states to be a generalization of squeezed states.

II. MOTIVATION FOR THE MODEL

One obvious generalization of squeezed states comes from recognizing that coherent states and squeezed states can be generated from idealized one-photon and two-photon devices, respectively.

We restrict our attention to a single mode of the electromagnetic field, at frequency ω, which can be represented by the harmonic oscillator annihilation and creation operators (a and $a^\dagger$, respectively.) In the Schrödinger picture the Hamiltonians for ideal one-photon and two-photon devices are given by

$$H_1=\omega a^\dagger a+i[z_1(t)a^\dagger-z_1^*(t)a]\ , \tag{2.1}$$

$$H_2=\omega a^\dagger a+i[z_2(t)a^{\dagger 2}-z_2^*(t)a^2]\ , \tag{2.2}$$

where

$$z_1(t)=|z|\exp[i(\phi-\omega t)]\ , \tag{2.3}$$

$$z_2(t)=|z|\exp[i(\phi-2\omega t)]\ , \tag{2.4}$$

are time-dependent complex coupling constants. Throughout the following, unless we write $\hbar$ explicitly we shall use units for which $\hbar=1$. We have chosen the time dependence of the couplings z_1 and z_2 so that, in the interaction picture, the Hamiltonians are independent of time; this corresponds to running the devices at resonance.

In the interaction picture the time evolution operators are

$$U_1=\exp[(za^\dagger-z^*a)t]\ , \tag{2.5}$$

$$U_2=\exp[(za^{\dagger 2}-z^*a^2)t]\ , \tag{2.6}$$

where $z=|z|\exp(i\phi)$ is a time-independent coupling constant. The operators U_1 and U_2 correspond to the displacement operator and the squeezing operator, respectively. U_1 and U_2 are already time ordered here since H_1 and H_2 are time independent in this picture.

In this paper we study an idealized degenerate k-photon parametric amplifier, which reduces to Eqs. (2.1) and (2.2) for $k=1$ and $k=2$, respectively. In the Schrödinger picture its Hamiltonian is

$$\begin{aligned}H_k&=\omega a^\dagger a+i[z_k(t)a^{\dagger k}-z_k^*(t)a^k]\\&\sim\omega a^\dagger a+2|z|\sin(k\omega t-\phi)E^k\ ,\end{aligned} \tag{2.7}$$

where $z_k(t)=|z|\exp[i(\phi-k\omega t)]$. The second form in Eq. (2.7) requires the rotating-wave approximation, and we have taken the electric field operator to be

$$E\sim(a^\dagger+a)\ . \tag{2.8}$$

For the rest of the paper we shall work in the interaction picture, so the time evolution operator corresponding to Eq. (2.7) is

$$U_k(z,z^*;t)=\exp[(za^{\dagger k}-z^*a^k)t]\ , \tag{2.9}$$

where $z\equiv|z|\exp(i\phi)$.

The second form in Eq. (2.7) allows the classical interpretation for the interaction as a nonlinear force oscillating at k times the natural frequency of the optical mode to which it is coupled. (For $k=1$ this is resonant excitation. For $k=2$ this is like kicking on a swing, where we force at twice the fundamental frequency.) This will excite the mode where its phase differs by $0,\ldots,2\pi(k-1)/k$ radians from the phase of the "force" $z_k(t)$ and damp it at the intermediate phases. Thus for $k>1$ we may expect this interaction to produce phase dependent noise.

Equation (2.7) also suggests a realization of the interaction, for which we make use of the macroscopic description for the electromagnetic field with matter; this is given by the polarizability

$$P_i=\chi_{ij}^{(1)}E_j+\chi_{ijm}^{(2)}E_jE_m+\cdots\ . \tag{2.10}$$

Here $\chi_{ij}^{(1)}$ is the first-order susceptibility of the material (which is simply $\chi^{(1)}\delta_{ij}$ for an isotropic material), $\chi^{(n)}$ is the nth-order nonlinear susceptibility, and the subscripts correspond to spatial and optical polarization components. The electromagnetic energy density is

$$\frac{1}{8\pi}\sum_i[(E_i+4\pi P_i)E_i+\text{ magnetic terms}]\ , \tag{2.11}$$

which from the decomposition in Eq. (2.8) has terms

$$\omega a^\dagger a+\cdots+\tfrac{1}{2}\chi^{(k)}(a^{\dagger k}+a^k)E_{\text{ext}}(t)+\cdots\ , \tag{2.12}$$

where E_{ext} is an external "pump" field, and we have ignored all but one spatial component and one optical polarization. A comparison with Eq. (2.7) yields

$$z(t)\sim\frac{-i}{2}\chi^{(k)}E_{\text{ext}}(t)V\ , \tag{2.13}$$

where V is the volume factor corresponding to the volume of the nonlinear material. (Similar terms arise from higher-order susceptibilities.)

This discussion shows how the model interaction in Eq. (2.7) may be formed by a kth-order (or higher) susceptibility. Of course, as Eq. (2.7) is only a model for such interactions, some details are left out. We have assumed an ideal pump for which there is no depletion. We neglect depletion since we only expect significant nonlinearities for very intense sources. We are also neglecting the dissipation and fluctuations that go with the mode being coupled to a thermal bath. Finally, we are glossing over the microscopic nature of the nonlinearity and quantizing directly the macroscopic equations of classical electromagnetism.

III. ANALYTIC PROPERTIES

Throughout this paper we are interested in the properties of the states generated from the interactions of Eq. (2.7). To describe these properties we shall make use of a quantum description which is closely linked to the phase-space distribution for a classical system.

The description we use, called the Q-function, is itself a probability distribution whose moments give "antinormally" ordered expectation values[9]

$$\langle a^n a^{\dagger m}\rangle\equiv\text{tr}[a^n a^{\dagger m}\rho(t)]=\int\frac{d^2\alpha}{\pi}\alpha^n\alpha^{*m}Q(\alpha,\alpha^*;t)\ , \tag{3.1}$$

where $d^2\alpha\equiv d\text{Re}(\alpha)d\text{Im}(\alpha)$, and

$$\rho(t)=U_k(t)\rho(0)U_k^\dagger(t)\ . \tag{3.2}$$

Here $U_k(t)$ is the time evolution operator [Eq. (2.9)] for our k-photon device, and $\rho(t)$ is the density operator for the state which determines the Q-function via[9,10]

$$Q(\alpha,\alpha^*;t)\equiv\langle\alpha\,|\,\rho(t)\,|\,\alpha\rangle=\text{tr}[\rho(t)\delta(a-\alpha)\delta(a^\dagger-\alpha^*)]\ , \tag{3.3}$$

where $|\alpha\rangle$ is the harmonic oscillator coherent state, $a\,|\alpha\rangle=\alpha\,|\alpha\rangle$. Equation (3.3) may be inverted to give

$$\rho(t)=\int\frac{d^2\alpha}{\pi}\delta(a^\dagger-\alpha^*)\delta(a-\alpha)Q(\alpha,\alpha^*;t)\ . \tag{3.4}$$

The expressions with operator-valued Dirac-delta functions may be considered as purely formal expressions for repeated Fourier transformations; we may write them as

$$\delta(a^\dagger-\alpha^*)\delta(a-\alpha)\equiv\int\frac{d^2\xi}{\pi}\exp[i\xi(a^\dagger-\alpha^*)]\exp[i\xi^*(a-\alpha)]\ , \tag{3.5}$$

$$\delta(a-\alpha)\delta(a^\dagger-\alpha^*)\equiv\int\frac{d^2\xi}{\pi}\exp[i\xi^*(a-\alpha)]\exp[i\xi(a^\dagger-\alpha^*)]\ .$$

The Q-function also represents[11] the joint probability distribution for a specially set up and balanced detector making simultaneous measurements of "position" $a^\dagger+a$ and "momentum" $i(a^\dagger-a)$. Hence we shall refer to contour plots of Q on $\text{Im}(\alpha)$ versus $\text{Re}(\alpha)$ as "phase-space" diagrams.

Let us define the rotation operator

$$R(\Theta)\equiv\exp(-i\Theta a^\dagger a)\ ; \tag{3.6}$$

then

$$R(\Theta)\,|\,\alpha\rangle=|\,\alpha e^{-i\Theta}\rangle\ , \tag{3.7}$$

and

$$a_\Theta\equiv R^\dagger(\Theta)aR(\Theta)=ae^{-i\Theta}\ . \tag{3.8}$$

Applying this rotation to $\rho(t)$ is equivalent to taking $\alpha\rightarrow\alpha\exp(-i\Theta)$ in $Q(\alpha,\alpha^*;t)$, which corresponds to rotation of the phase-space diagram. Also $R(\Theta)$ transforms the time evolution operator $U_k(t)$ to

$$R^\dagger(\Theta)U_k(t)R(\Theta)=\exp[(ze^{ik\Theta}a^{\dagger k}-z^*e^{-ik\Theta}a^k)t]\ , \tag{3.9}$$

i.e., $z\rightarrow z\exp(ik\Theta)$. When the initial state is the vacuum, $\rho(0)=|\,0\rangle\langle 0\,|$, a rotation by $\Theta=2\pi/k$ maps Q to itself, so that the phase-space plot will have a k-fold symmetry. This is familiar for $k=1$ and $k=2$, the coherent and squeezing cases.

For convenience, we shall henceforth restrict the coupling constant z to be real; when the initial state is the vacuum, this corresponds simply to a rotation of the phase-space diagram. We may now define a scaled time, $r\equiv|\,z\,|\,t$, so that the time evolution operator reduces to

$$U_k(r)=\exp[r(a^{\dagger k}-a^k)]\ . \tag{3.10}$$

We now derive the evolution equation for the Q-function. Although this is standard,[10] we present it for completeness. We start with the equation of motion for the density operator in the interaction picture:

$$i\frac{d\rho}{dt}=i\,|\,z\,|\,[a^{\dagger k}-a^k,\rho]\ . \tag{3.11}$$

Using the last expression in Eq. (3.3) and the relations

$$[a,\delta(a^\dagger-\alpha^*)]=\left\{\frac{\partial}{\partial a^\dagger}\delta(a^\dagger-\alpha^*)\right\}=-\frac{\partial}{\partial\alpha^*}\delta(a^\dagger-\alpha^*)\ , \tag{3.12}$$

$$[a^\dagger,\delta(a-\alpha)]=\left\{-\frac{\partial}{\partial a}\delta(a-\alpha)\right\}=\frac{\partial}{\partial\alpha}\delta(a-\alpha)\ , \tag{3.13}$$

$$a\delta(a-\alpha)=\alpha\delta(a-\alpha)\ , \tag{3.14}$$

$$a^\dagger\delta(a^\dagger-\alpha^*)=\alpha^*\delta(a^\dagger-\alpha^*)\ , \tag{3.15}$$

we find that the Q-function evolves according to

$$\frac{\partial Q}{\partial r}=LQ\equiv\left[\alpha^k-\left(\alpha+\frac{\partial}{\partial\alpha^*}\right)^k+\alpha^{*k}-\left(\alpha^*+\frac{\partial}{\partial\alpha}\right)^k\right]Q\ , \tag{3.16}$$

where L is the Liouvillian. Equation (3.16) has the formal solution

$$Q(r)=e^{rL}Q(0)=Q(0)+LQ(0)r+\tfrac{1}{2}L^2Q(0)r^2+\cdots\ , \tag{3.17}$$

where $Q(0)$ is the initial value of the Q-function.

If we treat this perturbation series for $Q(r)$ as an asymptotic series (Sec. V), then it is indeed valid to truncate the series to find the asymptotic behavior for small time. For the initial state in the vacuum $\rho(0)=|0\rangle\langle 0|$, corresponding to $Q(0)=\exp(-|\alpha|^2)$, we find

$$\begin{aligned}Q(r)&\sim e^{-|\alpha|^2}[1+r(\alpha^k+\alpha^{*k})]+O(r^2)\\&=e^{-|\alpha|^2}[1+2r|\alpha|^k\cos(k\theta)]+O(r^2)\ ,\end{aligned} \tag{3.18}$$

where $\alpha=|\alpha|e^{-i\theta}$. Thus, for $r\ll 1$, the Q-function develops k lobes along $\theta=0,2\pi/k,\ldots,2\pi(k-1)/k$ and dips between these lobes. We shall see later (Sec. V) that this is in agreement with more detailed calculations and even for such short times is different from the classical behavior (Sec. IV).

Similarly, if we start in an initial coherent state with real amplitude x_0, so that $\rho(0)=|x_0\rangle\langle x_0|$ and $Q(0)=\exp(-|\alpha-x_0|^2)$, then to first order in r,

$$Q(r)\sim e^{-|\alpha-x_0|^2}[1+r(\alpha^k+\alpha^{*k}-2x_0^k)]+O(r^2)\ ,$$

and for $x_0\gg|\alpha-x_0|$,

$$Q(r)\sim\exp\left[-\frac{[\mathrm{Re}(\alpha)-x_0-rkx_0^{k-1}]^2}{1+rk(k-1)x_0^{k-2}}-\frac{[\mathrm{Im}(\alpha)]^2}{1-rk(k-1)x_0^{k-2}}\right]+O(r^2)\ . \tag{3.19}$$

Thus, $\mathrm{Re}(\alpha)$ and $\mathrm{Im}(\alpha)$ have mean values and uncertainties given by

$$\sigma_{\mathrm{Re}(\alpha)}\sim\frac{1}{\sqrt{2}}\left[1+\frac{r}{2}k(k-1)x_0^{k-2}\right]+O(r^2)\ , \tag{3.20}$$

$$\sigma_{\mathrm{Im}(\alpha)}\sim\frac{1}{\sqrt{2}}\left[1-\frac{r}{2}k(k-1)x_0^{k-2}\right]+O(r^2)\ , \tag{3.21}$$

$$\langle\mathrm{Re}(\alpha)\rangle\sim x_0+rkx_0^{k-1}+O(r^2)\ , \tag{3.22}$$

$$\langle\mathrm{Im}(\alpha)\rangle\equiv 0\ , \tag{3.23}$$

for $r\ll 1$; the standard deviations $\sigma_{\mathrm{Re}(\alpha)}$ and $\sigma_{\mathrm{Im}(\alpha)}$ are independent of x_0 only for $k=1$ and $k=2$. For $k=3$, a resonant three-photon parametric amplifier will initially squeeze an in-phase coherent state at a rate proportional to its amplitude. Also there would be no ordinary squeezing of the vacuum for any of the $k>2$ processes. Similar results have been obtained by Hillery, Zubairy and Wódkiewicz.[12] They have also shown that this generalized parametric amplifier produces no ordinary squeezing of the vacuum when $k>2$, even for large r.

IV. CLASSICAL DYNAMICS

It is worthwhile calculating the classical dynamics associated with the interaction in Eq. (2.7) in detail, not only to confirm our intuition from Sec. II, but also to compare it to the full quantum dynamics.

There is not always, however, a unique classical system that one might associate with a quantum Hamiltonian. In order to choose a classical Hamiltonian, we start by writing the quantum theory in terms of a path integral; the classical Hamiltonian then appears as part of the classical action in the path integral. Another route to the classical Hamiltonian may be found in Milburn.[13]

In the coherent state representation of Klauder,[14] the full propagator is

$$\langle\alpha_f;t\,|\,\alpha_i;0\rangle=\int_{\alpha(0)=\alpha_i}^{\alpha(t)=\alpha_f}D(\alpha(\tau))\exp\left[\int_0^t d\tau[\tfrac{1}{2}(\alpha\dot{\alpha}^*-\alpha^*\dot{\alpha})-iH_N(\alpha^*,\alpha;\tau)]\right]\ , \tag{4.1}$$

where $D(\alpha(\tau))$ is the path integral measure, and

$$\begin{aligned}H_N(\alpha^*,\alpha;t)&\equiv\langle\alpha|H(t)|\alpha\rangle\\&=\omega|\alpha|^2+i|z|(\alpha^{*k}e^{-ik\omega t}-\alpha^k e^{ik\omega t})\ ,\end{aligned} \tag{4.2}$$

is the appropriate classical Hamiltonian, which is just the quantum Hamiltonian in normal order form, with a replaced by α and $a^\dagger$ by α^*. The Poisson bracket then yields the classical equation of motion

$$\frac{\partial Q_{\mathrm{cl}}}{\partial t}=-\{H_N,Q_{\mathrm{cl}}\}=i\frac{\partial H_N}{\partial\alpha^*}\frac{\partial Q_{\mathrm{cl}}}{\partial\alpha}-i\frac{\partial H_N}{\partial\alpha}\frac{\partial Q_{\mathrm{cl}}}{\partial\alpha^*}\ , \tag{4.3}$$

where Q_{cl} is the classical probability distribution in phase space.

In a rotating frame (analogous to the interaction picture), the classical equation (after scaling out the coupling constant $|z|$) is therefore

$$\frac{\partial Q_{\mathrm{cl}}}{\partial r}=-k\left[\alpha^{k-1}\frac{\partial Q_{\mathrm{cl}}}{\partial\alpha^*}+\alpha^{*-1}\frac{\partial Q_{\mathrm{cl}}}{\partial\alpha}\right]\ . \tag{4.4}$$

It has the asymptotic dynamics

$$Q_{\mathrm{cl}}=e^{-|\alpha|^2}[1+2kr|\alpha|^k\cos(k\theta)]+O(r^2)\ , \tag{4.5}$$

for an initial Q_{cl} that corresponds to Q for the vacuum, i.e., $Q_{\mathrm{cl}}=\exp(-|\alpha|^2)$. The lobes of Q_{cl} grow k times faster than the corresponding quantum features [see Eq. (3.18)], at least for $r\ll 1$.

We can make an interesting general observation about these classical equations of motion at this point. Writing

the quantum equation of motion in terms of $H_N(\alpha^*,\alpha)$, we have

$$i\frac{\partial Q}{\partial t}=H_N\left[\alpha^*,\alpha+\frac{\partial}{\partial\alpha^*}\right]Q-QH_N\left[\alpha^*+\frac{\overleftarrow{\partial}}{\partial\alpha},\alpha\right] \tag{4.6}$$

$$=\frac{\partial H_N}{\partial\alpha}\frac{\partial Q}{\partial\alpha^*}-\frac{\partial H_N}{\partial\alpha^*}\frac{\partial Q}{\partial\alpha}+(\text{higher derivatives of } Q)\,, \tag{4.7}$$

where the derivative $\overleftarrow{\partial}/\partial\alpha$ acts to the left. Thus, truncating the full quantum description of Eq. (4.6) to first order in the derivatives of Q leads us to the same classical equation we derived from the path integral formulation [Eq. (4.3)]. This truncation obviously leads to classical dynamics, and the classical trajectories are given by solving the characteristic equations for the resulting first order partial differential equation. These characteristic equations (classical trajectories) for Eq. (3.16) are

$$\frac{d\alpha}{dr}=k\alpha^{*k-1}\,, \tag{4.8}$$

$$\frac{d\alpha^*}{dr}=k\alpha^{k-1}\,. \tag{4.9}$$

These classical trajectories conserve

$$H_N\propto\frac{i}{2}(\alpha^{*k}-\alpha^k)\,, \tag{4.10}$$

so the classical trajectories are curves of constant $\mathrm{Im}(\alpha^k)$. These curves describe a flow in phase space around an unstable fixed point with k directions of damping and k directions of growth. Thus the Hamiltonian has a k-saddle around the unstable fixed point. This is a generalization of the generic saddle of unstable fixed points.

Integrating the characteristic equations numerically, for $k=3$, gives Figs. 1(a) and 1(b); the threefold symmetry and the development of lobe structure are apparent. We also see that arbitrarily sharp structure appears as r increases. This sharp structure is a feature of the classical dynamics of many systems.[15] We do not expect to see it in the quantum system, for as it develops the higher derivatives become significant. For instance, the sharp structure develops along the lines $\theta=0,2\pi/k,\ldots,2\pi(k-1)/k$; so expanding Eq. (4.4) about $\theta=0$ with

$$|\alpha|\gg\max\left[1,\frac{1}{|\alpha|}\left|\frac{\partial Q}{\partial\theta}\right|\right],$$

and

$$\frac{1}{|\alpha|}\left|\frac{\partial Q}{\partial\theta}\right|\gg\left|\frac{\partial Q}{\partial|\alpha|}\right|\,, \tag{4.11}$$

one finds that for any k the term that dominates is the diffusion term, leading to the equations

$$\frac{\partial Q}{\partial r}=\tfrac{1}{4}k(k-1)|\alpha|^{k-2}\left[\frac{1}{|\alpha|^2}\frac{\partial^2 Q}{\partial\theta^2}\right]. \tag{4.12}$$

We see that this diffusion term vanishes for $k=1$ and is independent of $|\alpha|$ for $k=2$. For $k>2$, it is proportional to $|\alpha|^{k-2}$; thus any attempt to squeeze at a faster rate as suggested at the end of Sec. III will have to fight this diffusion. Numerical results suggest that even for $k=4$ this diffusion dominates.

It is worth noting that this "quantum diffusion" is not the only way quantum mechanics may prevent fine structure being formed by the classical evolution. Milburn[13] has studied a different nonlinear potential which produces a negative-definite diffusion term; it prevents the classical structure by forcing recurrences of the initial state.

V. QUANTUM DYNAMICS

There are at present no analytic techniques for dealing with the full problem. One obvious method would be to normal order the evolution operator U_k [Eq. (3.10)]; however, for $k>2$ this is an unsolved problem.[16] Fisher, Nieto, and Sandberg[7] look at the matrix element

$$\langle 0|U_k(r)|0\rangle=1-\frac{k!}{2!}r^2+\frac{(k!)^2+(2k)!}{4!}r^4-\frac{(k!)^3+2k!(2k)!+(2k)!^2/k!+(3k)!}{6!}r^6+\cdots+(-1)^n\frac{(nk)!}{(2n)!}C_nr^{2n}+\cdots \tag{5.1}$$

by expanding it as a Taylor series in r. All the coefficients C_n are positive. They point out that this series has a zero radius of convergence; in fact, the coefficients C_n grow like β^n, where $\beta(k)$ is near 1. Thus, the vacuum state is by definition[17] a nonanalytic vector with respect to the Hamiltonian H_k. This does not, however, reflect on the existence of the Hamiltonian, as they imply, or on the unitarity of U_k. The nonconvergence is in fact a mathematical artifact caused by singular behavior on the imaginary time axis, since Taylor series converge only up to the nearest pole. (This phenomenon is quite common in parabolic equations; for example, the initial value problem for the heat equation has no solution for negative time.)

There are many methods of analytic continuation available which obtain useful information from Taylor series outside their radius of convergence. If that radius is actually zero, then we can still hope to extract information by deriving an alternative form which does converge, since in this case the Taylor expansion would be an asymptotic series about $r=0$. One such method is that of Padé approximants,[18,19] in which the $[N/M]$ approximant is a rational function $P_M^N(r^2)=P_N(r^2)/Q_M(r^2)$, where P_N (Q_M) is a polynomial of degree N (M). The coefficients of the polynomials P_N and Q_M are chosen so as to match the first $M+N+1$ Taylor coefficients of the function. (Q_M has leading coefficient 1.) Padé approximants analytically continue well because they tend to reproduce the pole structure that limits the Taylor series' convergence. A

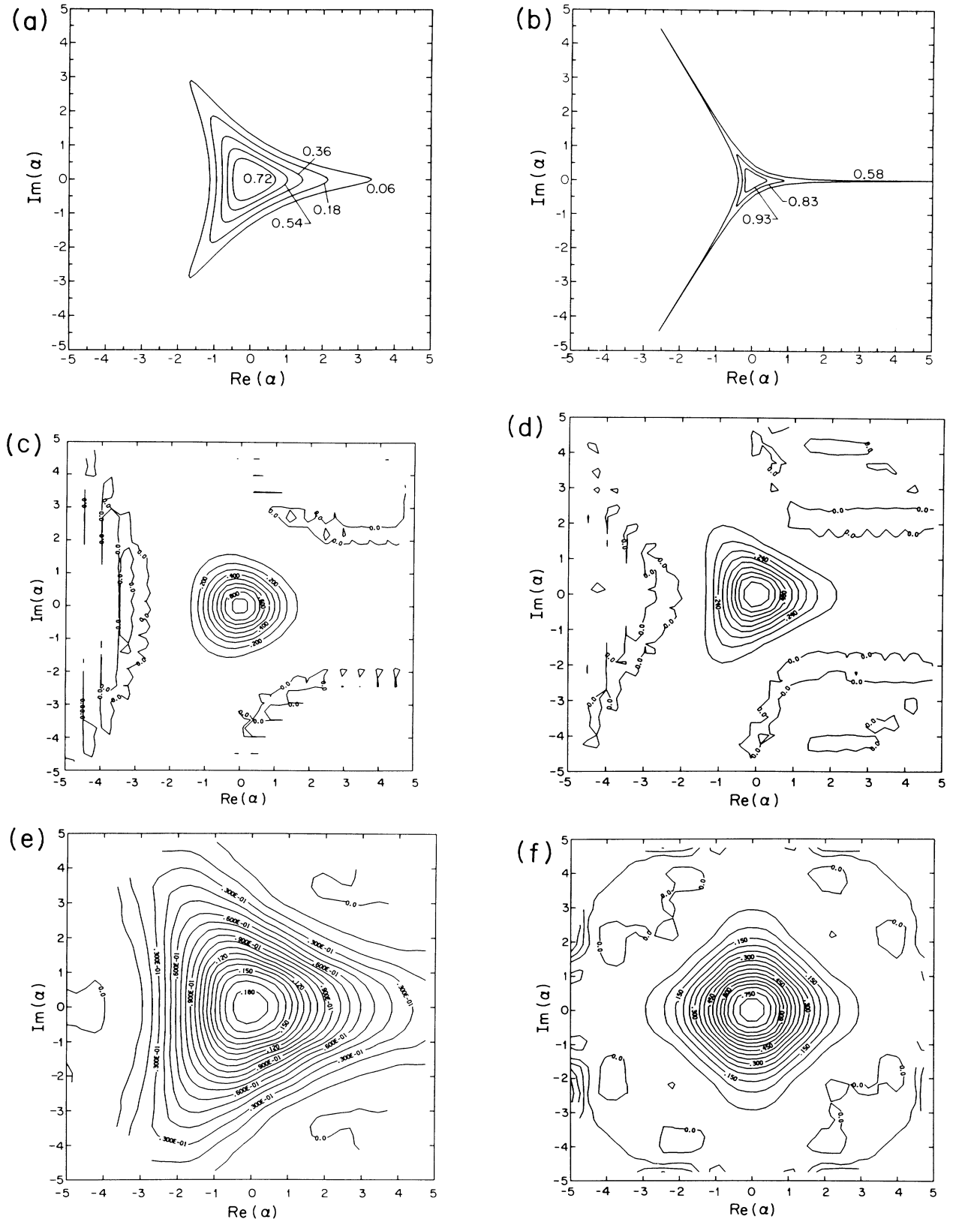

FIG. 1. (a) and (b) Contour plots of the classical phase-space distribution, $Q_{\rm cl}(r)$, for $k=3$, at times (a) $r=0.05$ and (b) $r=0.2$. (c)—(f) Contour plot of the quantum Q-function, $Q(r)$, for (c) $r=0.05$ and $k=3$; (d) $r=0.2$ and $k=3$; (e) $r=1.0$ and $k=3$; and (f) $r=0.1$ for $k=4$.

common application is to form a diagonal series from the $[N/N]$ and $[N/N+1]$ approximants (these require $2N+1$ and $2N+2$ coefficients respectively); this often has remarkable convergence properties. We restrict our attention to this series.

In practice, one represents the rational function as a continued fraction. Surprisingly, this means that successive Padé approximants can be calculated by generating only one additional continued-fraction coefficient.[18] This breaks down if there is a zero Taylor coefficient. Hence, we regard Eq. (5.1) as an expansion in r^2; i.e. we analytically continue in r^2 instead of r. The algorithms tend to be numerically sensitive—about half a digit is lost for every extra term required—so we worked in high precision throughout (~ 33 significant figures, with checks at even higher accuracy). This is not a problem with Padé approximants, but rather a characteristic of the numerical treatment of analytic continuation methods in general, which try to predict behavior far from the origin from the first few terms of the Taylor series. For instance, in this case to perform Borel summability instead of Padé approximation requires the numerical integration of rapidly oscillating functions.

For $k=1$ and $k=2$, the series of Padé approximants converges rapidly to the known solutions

$$\langle 0 \mid U_1(r) \mid 0 \rangle = \exp(-r^2/2) , \tag{5.2}$$

$$\langle 0 \mid U_2(r) \mid 0 \rangle = \cosh^{-1/2}(2r) . \tag{5.3}$$

For $k=3$, we see convergence out to $r \sim 1.2$ [see Fig. 2(a)]. One reason for this is that the first 56 continued fraction coefficients are all positive, which gives the relations[18]

$$P^N_{N+1} \leq P^{N+1}_{N+2} \leq P^{N+1}_{N+1} \leq P^N_N \tag{5.4}$$

for $2N+2 \leq 56$; i.e., the odd and even Padé approximants bracket their limit [see Fig. 2(b)].

P^N_M in general has M simple poles, some of which mimic the real poles of the function and some of which are spurious. The convergence of the approximants will then depend on whether the spurious poles are eventually canceled by zeros in the numerator or move off to infinity as N and $M \to \infty$. In our case the poles initially lie on the negative real axis (corresponding to imaginary r), clustering close to zero; this is the usual behavior on a branch cut. However, coefficients 57, 58, and 168 are negative which introduces spurious poles. These prevent convergence for large r unless enough terms are included to move the pole well past r [see Figs. 2(b) and 3].

We repeated these calculations for different matrix elements, enabling us to compute the Q-function. For a system initially in the vacuum state, $\rho(0) = \mid 0 \rangle \langle 0 \mid$, a decomposition in the number state basis yields

$$Q(r) = \exp(-\mid \alpha \mid^2) \left| \sum_{n=0}^{\infty} \frac{\alpha^{*n}}{\sqrt{n!}} \langle n \mid U_k(r) \mid 0 \rangle \right|^2 . \tag{5.5}$$

We note that the finiteness of the vacuum-to-vacuum matrix element of Eq. (5.1) determines the finiteness of all the other matrix elements in the sum of Eq. (5.5). This is because these matrix elements are nonzero only when n is a multiple of k, in which case they can be written as sums of derivatives of the vacuum-to-vacuum matrix element:

$$\langle k \mid U_k(r) \mid 0 \rangle = \frac{1}{\sqrt{k!}} \frac{d}{dr} \langle 0 \mid U_k(r) \mid 0 \rangle ,$$

$$\langle 2k \mid U_k(r) \mid 0 \rangle = \frac{1}{\sqrt{(2k)!}} \left[k! + \frac{d^2}{dr^2} \right] \langle 0 \mid U_k(r) \mid 0 \rangle , \tag{5.6}$$

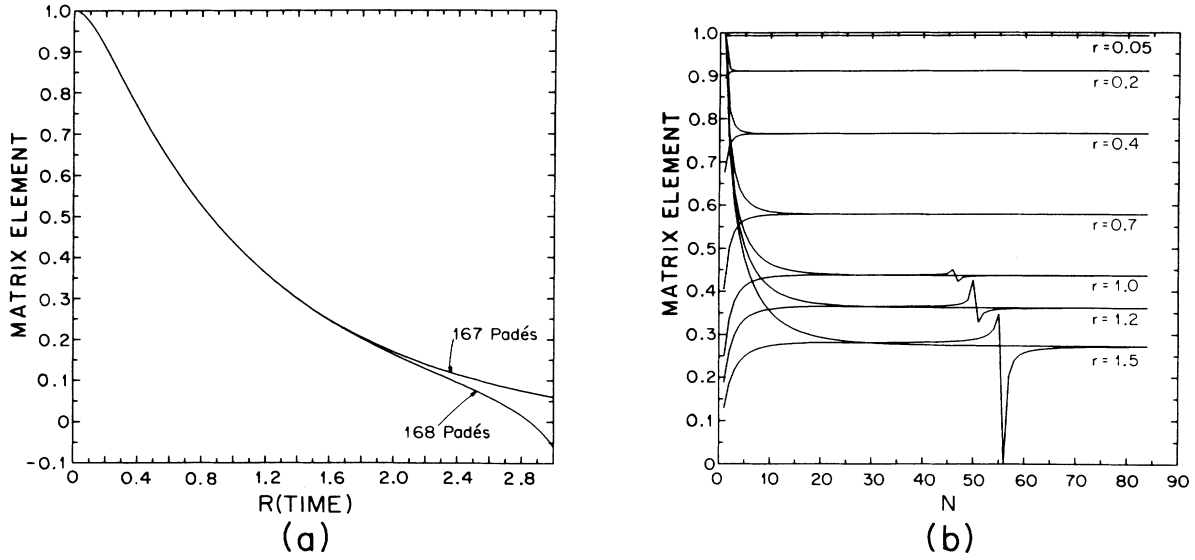

FIG. 2. (a) Plot of the matrix element, $\langle 0 \mid U_{k=3}(r) \mid 0 \rangle$, versus scaled time r, when calculated with $2N+1=167$ and $2N+2=168$ Padé coefficients. This shows convergence of the matrix element out to $r \sim 1.2$. (b) Plot of the value of the matrix element, $\langle 0 \mid U_{k=3}(r) \mid 0 \rangle$, versus N, for various times: $r=0.05$; $r=0.2$; $r=0.4$; $r=0.7$; $r=1.0$; $r=1.2$; and $r=1.5$. P^N_N and P^N_{N+1} are plotted separately to show how they bracket their "limit" until they reach the spurious pole at $2N+2=58$. We also see that the spurious pole moves out to higher times as N is increased.

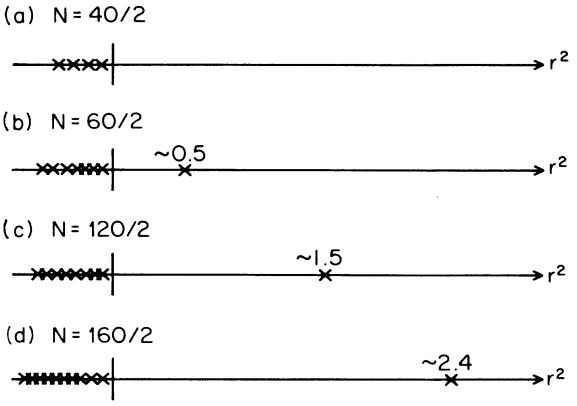

FIG. 3. Schematic plot of the positions of the poles in the Padé approximant to $\langle 0 \mid U_{k=3}(r) \mid 0 \rangle$ as a function of r^2, for (a) $2N+2=40$; (b) $2N+2=60$; (c) $2N+2=120$; and $2N+2=160$. This shows the accumulation of poles near the origin (for $r^2<0$) which causes the difficulty with convergence of the Taylor series. It also shows the motion of the spurious pole, as in Fig. 2(b).

etc. Now $|\langle n \mid U_k(r) \mid 0 \rangle|^2$ is a probability so it is bounded above by 1. Thus the sum in Eq. (5.5) converges rapidly; e.g., for $\alpha \lesssim 5$ we only need to include terms up to $n=74$ (this corresponds to only 25 nonzero terms for $k=3$) in the sum for each additional term to give a contribution of less than one percent. The contour plots of the Q-function are shown in Figs. 1(c)–1(e) for $r=0.05$, 0.2, and 1.0. Notice the threefold symmetry and the lobe development, which is much slower and wider than in the classical case (Secs. III, IV). Our techniques also work for higher k [see Fig. 1(f) for $k=4$], but the numerical problems become more extreme.

As a final point we calculated two of Hong and Mandel's[8] "higher-order squeezing" parameters, $\langle :(\Delta a_{\Theta 1})^{2n}: \rangle$, for the quantum states in Figs. 1(c)–1(f). Here the colons denote normal ordering, and $a_{\Theta 1}=a_\Theta+a_\Theta^\dagger$ is the quadrature amplitude defined at an angle Θ to the Re(α) axis [Eq. (3.8)]. Using the P representation[9,10]

$$P(\alpha,\alpha^*)=\mathrm{tr}[\rho(t)\delta(a^\dagger-\alpha^*)\delta(a-\alpha)] , \tag{5.7}$$

which generates the expectation values of normally ordered operators, and the relation for reordering the Dirac-delta functions

$$\delta(a^\dagger-\alpha^*)\delta(a-\alpha)=\exp\left[-\frac{\partial^2}{\partial\alpha\partial\alpha^*}\right]\delta(a-\alpha)\delta(a^\dagger-\alpha^*) , \tag{5.8}$$

we find

$$P(\alpha,\alpha^*)=\exp\left[-\frac{\partial^2}{\partial\alpha\partial\alpha^*}\right]Q(\alpha,\alpha^*) . \tag{5.9}$$

Hence, the normally ordered "squeezing" parameter becomes

$$\begin{aligned}\langle :(\Delta a_{\Theta 1})^{2n}: \rangle &= \int \frac{d^2\alpha}{\pi} P(\alpha,\alpha^*)(\alpha_\Theta+\alpha_\Theta^*-\langle a_{\Theta 1}\rangle)^{2n} \\ &= \int \frac{d^2\alpha}{\pi} Q(\alpha,\alpha^*)\exp\left[-\frac{\partial}{\partial\alpha\partial\alpha^*}\right] \\ &\quad\times(\alpha_\Theta+\alpha_\Theta^*-\langle a_{\Theta 1}\rangle)^{2n} ,\end{aligned} \tag{5.10}$$

after integration by parts.

These parameters are trivially positive for classical states, and Hong and Mandel call a state squeezed to $2n$th order if $\langle :(\Delta a_{\Theta 1})^{2n}: \rangle$ is negative. In each case described in Figs. 1(c)–1(f), we calculated this parameter for $n=1$ and $n=2$, with $\Theta=0,\pi/k$, and found it to be positive in each case; i.e., there is no fourth-order squeezing of the kind described by Hong and Mandel,[8] nor is there any ordinary squeezing for these states (ordinary squeezing occurs when their parameter for $n=1$ is negative). One reason why we might have expected this is that their parameters make use of an orthogonal decomposition of phase space into quadrature amplitudes; instead our states have a k-fold symmetry, which will not match this decomposition when $k>2$.

As pointed out by Fisher, Nieto, and Sandberg,[7] the self-adjointness and Hermiticity of the interaction Hamiltonian $H_k=i(za^{\dagger k}-z^*a^k)$ is not in question. What is questioned is the unitarity of the theory, but the only potential problem we see would be if the matrix elements of the time evolution operator $U_k(r)$ did not exist. We have demonstrated numerically that they do.

VI. CONCLUSIONS

We conclude that this generalization of "one-photon" coherent and "two-photon" squeezed states to "many-photon" states is possible and that these non-gaussian states show quantum features quite different from the classical approximation. These k-photon interactions for $k>2$ initially generate ordinary squeezing at a higher rate than the usual $k=2$ parametric amplifier when they act resonantly on a large amplitude coherent state. This occurs, however, in competition with a quantum diffusion which gets stronger for successively larger k.

ACKNOWLEDGMENTS

One of the authors (S.L.B.) would like to thank Carlton M. Caves for pointing out Ref. 7 and for many useful discussions on the physics, he also appreciates discussions with Daniel Neuhauser on high-precision calculations; and R.I.M. would like to thank Dan Meiron for discussions on analytic continuation. This work was supported in part by the Office of Naval Research [Contract No. N00014-85-K-0005]. R.I.M. was supported in part by the University Grants Committee of New Zealand.

[1]For a review see D. F. Walls, Nature **306**, 141 (1983).
[2]R. E. Slusher, L. W. Hollberg, B. Yurke, J. C. Mertz, and J. F. Valley, Phys. Rev. Lett. **55**, 2409 (1985).
[3]See A. L. Robinson, Science **233**, 280 (1986).
[4]C. M. Caves, Phys. Rev. D **23**, 1693 (1981).
[5]R. S. Bondurant and J. H. Shapiro, Phys. Rev. D **30**, 2548 (1984).
[6]B. Yurke, J. R. Klauder and S. L. McCall, Phys. Rev. D **33**, 4033 (1986).
[7]R. A. Fisher, M. M. Nieto and V. D. Sandberg, Phys. Rev. D **29**, 1107 (1984).
[8]C. K. Hong and L. Mandel, Phys. Rev. Lett. **54**, 323 (1985)
[9]K. E. Cahill and R. J. Glauber, Phys. Rev. **177**, 1882 (1969).
[10]W. H. Louisell, *Quantum Statistical Properties of Radiation* (Wiley, New York, 1973).
[11]E. Arthurs and J. L. Kelly, Jr., Bull. Syst. Tech. J. **44**, 725 (1965).
[12]M. Hillery, M. S. Zubairy and K. Wódkiewicz, Phys. Lett. **103A**, 259 (1984).
[13](a) G. J. Milburn, Phys. Rev. A **33**, 674 (1986); see also (b) G. J. Milburn and C. A. Holms, Phys. Rev. Lett. **56**, 2237 (1986).
[14]J. R. Klauder, Ann. Phys. (N.Y.) **11**, 123 (1960).
[15]M. V. Berry, in *Chaotic Behavior of Deterministic Systems, Les Houches Lectures, 1981,* edited by G. Iooss, R. H. G. Helleman, and R. Stora (North-Holland, Amsterdam, 1982).
[16]W. Witschell, Phys. Lett. **111A**, 383 (1985).
[17]E. Nelson, Ann. Math. **70**, 572 (1959).
[18]C. M. Bender and S. A. Orszag, *Advanced Mathematical Methods for Scientists and Engineers* (McGraw-Hill, New York, 1978), p.383.
[19]G. A. Baker, *Essentials of Padé Approximants* (Academic, New York, 1975).